Polymer Bulletin 33, 673–680 (1994)

Polymer Bulletin

Poly(vinylidene fluoride)/cellulose acetate-butyrate blends: Characterization by DSC, WAXS, and FTIR

Humberto Vázquez-Torres[*,1,2] **and Carlos A. Cruz-Ramos**[2,**]

[1] Depto. de Física, Universidad Autónoma Metropolitana-Iztapalapa (UAM-I), Apdo. Postal 55-534, México, D.F., México, 09340
[2] Depto. de Polímeros, Centro de Investigación Científica de Yucatán, A.C. (CICY), Apdo. Post. 87, Cordemex, Mérida, Yucatán, México, 97310

Summary

Binary blends of poly(vinylidene fluoride), PVDF, with cellulose acetate-butyrate (CAB) were characterized by using differential scanning calorimetry (DSC), wide angle X-ray scattering (WAXS) and Fourier transform infrared spectroscopy (FTIR). This system was proved to be partially miscible, showing a significant decrease on the thermal parameters (ΔH_f and T_m) as well as on the crystallinity index (CI) of PVDF with CAB content on the second DSC run. γ crystalline form of PVDF, which is predominant in the as-cast blends, changed to α form with the first DSC run. In contrast, thermal treatment at 200°C (30 min) on blends containing 40-60 wt. % of CAB caused the γ phase to be predominant, as observed by FTIR.

Introduction

PVDF is known to crystallize in a variety of crystal forms, which melt at different temperatures (1-7). The preferential development of these forms depends on the applied experimental conditions: annealing temperature, strong electric fields, compression, and combinations of these variables. α-, β- and γ-crystal forms are the most studied. The first one is non-polar and is present in commercial samples of PVDF, while β-crystals arise in PVDF annealed above 147°C or cast from DMF or DMAc solutions, and γ is nucleated from the melt. β- and γ-crystal forms are polar in nature and originate the piezo- and pyroelectric behavior of poled PVDF films. X-ray scattering, differential scanning calorimetry, infrared, polarized optical microscopy, and dielectric relaxation have been primarily applied to characterize this polymorphism of PVDF (1-11). On the other hand, PVDF has been reported to give miscible blends with other synthetic polymers (12-16). The driving force for miscibility in this system presumably arises from strong, specific interactions in which the highly polar vinylidene groups of PVDF and the carbonyl groups of PMMA are involved (16). PVDF also forms miscible blends with poly(vinyl alcohol), PVA, presumably as a result of the specific interactions of the vinylidene groups with the hydroxyl groups of PVA (13). Following this idea, blends of PVDF with cellulosic esters (CEs) are expected to exhibit certain degree of miscibility due to

* Corresponding author
** Present address: Röhm and Haas Co., P.O. Box 219, Bristol, PA 19007, USA

the possible occurrence of specific interactions between both components. Miscibility studies of cellulose and its derivatives with other polymers are scarce (19-21). This is partially due to the strong tendency of CEs to form hydrogen bonds with themselves, in which the non-substituted hydroxyls are the proton-donor groups and the carbonyls of esters behave as the proton-acceptor groups, as pointed out elsewhere (20). Although PVDF polymorphism has been extensively studied in this polymer alone, there are only a few reports on this behavior for blended PVDF in literature (17,22,23). This behavior was recently considered in calculations of the interaction parameter from melting-point depression for PVDF/PMMA blends (24). To our knowledge, there are only two blends, for which it has been reported that a low content of other polymer causes an increase on the extent of β form in PVDF, namely those with PMMA (22) and PVF (25).
In this work, miscibility studies on blends of PVDF with CAB are reported. DSC, WAXS, and FTIR techniques were used for characterizing these blends. DSC results indicate that the PVDF/CAB blend is, at least, partially miscible. WAXS and FTIR studies allow to follow the changes by the different crystal forms of PVDF when varying experimental conditions.

Experimental.

PVDF and CAB were purchased from Polysciences. CAB contains 17% of butyryl groups, i.e., 1.1 butyryl, 1.7 acetyl, and 0.2 hydroxyl groups per repeating unit. Molecular weights (M_W) are 42,000 for CAB and 100,000 for PVDF. Reagent-grade N,N-dimethylformamide (DMF) from Merck (México) was used as solvent. Polymers to be mixed were allowed to dissolve separately at room temperature in DMF. The resulting solutions, with 2 wt. % of polymers, were mixed together and stirred at room temperature for 4 h. Films of pure and blended polymers were obtained by casting these solutions at 50°C, and then drying them in a vacuum oven at 110°C for one week.
Samples (25-30 mg) of blended films were tested in duplicate using a Perkin-Elmer DSC-2C calorimeter calibrated with tin and indium. Large samples were required because the characteristic low signal at the glass transition temperature (T_g) showed by cellulose acetates. Three consecutive DSC runs were carried out on each sample of pure and blended polymers, from -60 to 240°C at 10°C/min and under a N_2 flux of 20 cc/min. Data acquisition and calcultaions were made with a 1600 Data Station (Perkin-Elmer) by using the TADS program (Perkin-Elmer). T_g and T_m were measured at the onset and at the maximum of endothermal peak of DSC traces, respectively. WAXS measurements were carried out on 0.1 mm thick films by using a horizontal goniometer Philips (Model PW-1140/60) which was coupled with CuKα target x-ray tube operated at 40 kV and 30 mA. Monocromatization was achieved by Bragg´s diffraction from a graphite crystal and intensity diffraction was recorded with a proportional counter coupled with a Ratemeter system, in the 2θ range from 5 to 60°, at 1°/min. FTIR studies were conducted on very thin films (10-20 μm thick)

with a FTIR (Perkin-Elmer 1600) spectrophotometer between 4000 and 200 cm^{-1}. Measurements were performed at room temperature on: a) the dried, as-cast films and, b) the same films after heated to 240°C and thermally treated at 200°C for 30 min and cooling to room temperature at 40°/min.

Results and Discussion.

Figure 1 reports typical DSC thermograms obtained for pure polymers (PVDF and CAB) and the 50/50 % blend. The DSC trace of the first run for pure PVDF shows an increase on ΔC_p at about 120°C, which has been atributed to melting of condis crystals (26), and an endothermal peak with a maximum at 164°C corresponding to T_m. Second run trace exhibits this T_m also at 164°C and the T_g at -10°C. For CAB, in turn, the DSC trace of the first run shows a T_g at 149°C and an endothermal peak at 227°C, indicating melting of crystals that had been formed during casting from DMF solution. The second DSC run on this pure CAB film exhibits the expected T_g at 149°C and a total disappearance of the endothermal peak at 227°C, which indicates that no further crystallization took place in CAB during cooling. Regarding the 50/50 % blend, it is worthy of notice that there is an endothermal peak at 206°C in the first run trace, which was not observed for the parent polymers. This peak does not appear in the second run, and a probable interpretation will be given below in the light of WAXS and FTIR results.

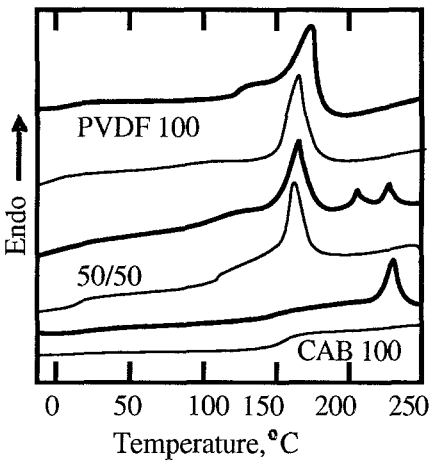

Fig.1. Typical DSC traces for PVDF/CAB blends: first run (▬) and second run (—). Numerals indicate blend composition.

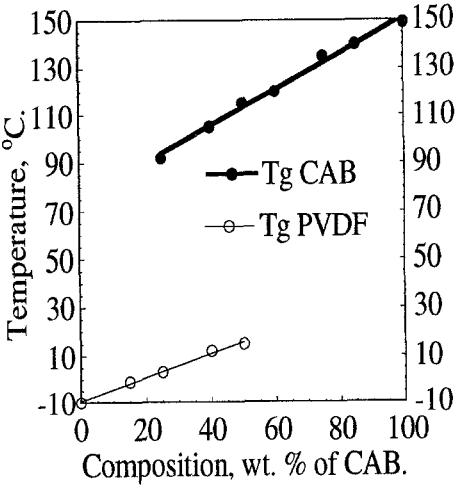

Fig.2. Dependence of T_g's for the PVDF/CAB blend with composition in the second run DSC traces.

Two T_g's are appreciated in DSC runs of the 50/50 % blend. That of PVDF is shifted up to 15°C, whilst that of CAB is shifted down to 110°C. This latter T_g is more clearly observed in the second run because the premelting of PVDF condis crystals are absent in this region. Based on both the absence of the premelting signal and the excellent reproducibility of the second and third runs, the second run traces were used for the discussion on the miscibility behavior of PVDF/CAB.

Figures 2, 3a, and 3b report the dependence of thermal events with composition for the all PVDF/CAB blends. The two T_g's in Figure 2 are shown to be composition-dependent, varying toward intermediate values. Also, it can be clearly observed that both enthalpy of fusion (ΔH_f) and melting point (T_m) of PVDF decrease drastically with the CAB content (Figs. 3a,b) in the second runs. At this point, it must be emphasized that ΔH_f values were normalized with respect to the PVDF weight content for each blend. Thus, an independence of ΔH_f on CAB content would result in an horizontal line in Fig. 3b. On the basis on these results, primarily on the variation of T_g's with composition, the PVDF/CAB blend is considered to be partially miscible.

WAXS diffractograms exhibit interesting changes for PVDF/CAB blends after heating under DSC conditions (up to 240°C) in contrast to those obtained for the as-cast blends (Fig. 4a). It was pointed out that the 2θ region from 17 to 21° (Fig. 4a) comprises scattering peaks of α-, β-, and γ-crystal forms, and that at $2\theta = 27°$ corresponds to α crystalline form (25).

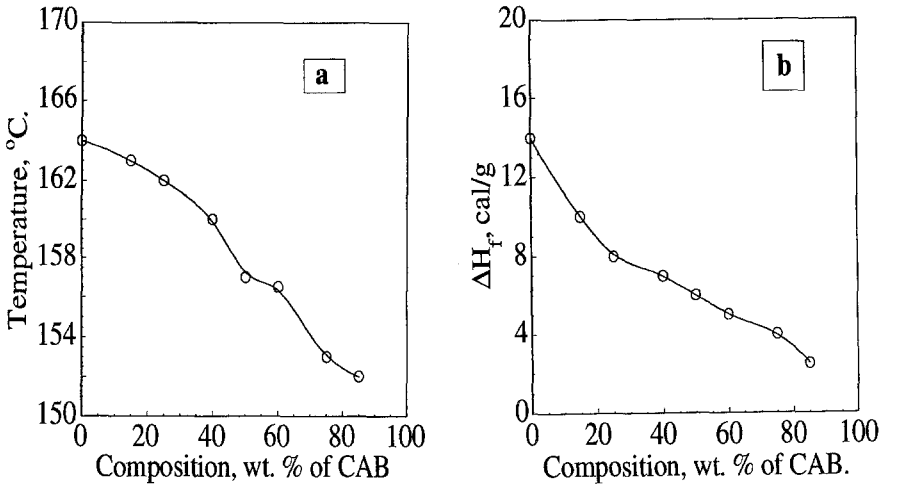

Fig. 3. Dependence of thermal parameters for PVDF/CAB system with blends composition, as observed in the second run DSC traces: (a) Melting-point, T_m, and (b) enthalpy of fusion, ΔH_f, for the crystalline phase of PVDF. ΔH_f was normalized with respect to the weight of PVDF contained in the blends.

As the diffractogram for the as-cast pure PVDF (Fig. 4a) does not show any peak at $2\theta = 27^{o}$, and is very similar in shape to that reported for PVDF containing essentially β-crystals (25), it may be assumed that α-crystals are practically absent in the as-cast PVDF. However, due to the fact that both β and γ forms scatter x-rays in the same region of WAXS diffractograms, it is not possible to distinguish them when both are present.

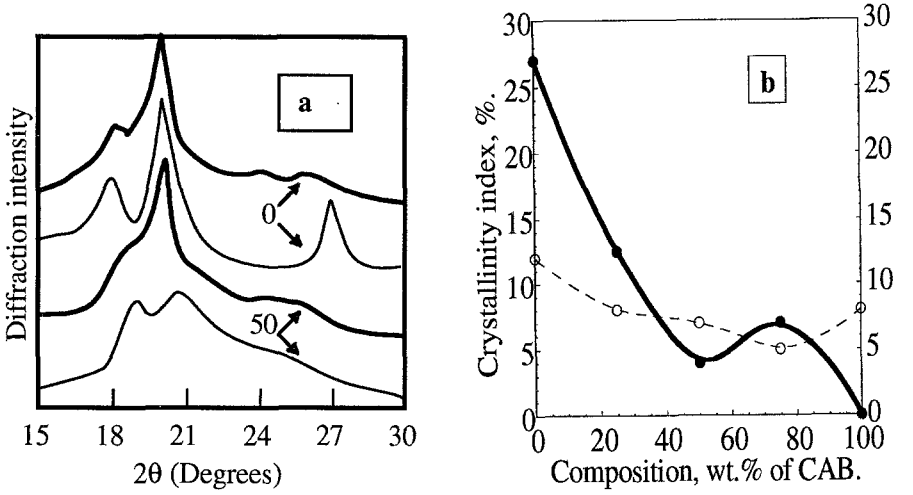

Fig. 4. (a) Typical WAXS diffractograms for the PVDF/CAB system: before (▬) and after (—) the first DSC run. (b) Crystallinity index for the same system: before (▬) and after (—) the first DSC run.

Table 1. Crystallinity index (CI) from WAXS for PVDF/CAB blends.

Blends	Composition (wt. %)				
	100/0	75/25	50/50	25/75	0/100
PVDF/CAB-1	11.0	8.0 (10.2)	7.0 (9.5)	5.0 (8.7)	8.0
PVDF/CAB-2	27.0	12.5 (20.2)	4.0 (13.5)	6.0 (6.7)	0.0

Values in parenthesis represent the CI that would be expected if the CAB had no effect on the PVDF. The numbers 1 and 2 mean that measurements were made before and after the first DSC run, respectively.

However, it is clear that heating under DSC conditions destroyed the β- or γ-crystals. Then, crystallization of PVDF yielded preferentially α-crystals, as a consequence of the higher thermodynamic stability of α-crystals at relatively

low crystallization temperature (140 - 162°C). In contrast, β- or γ-crystals are kinetically favored at temperatures higher than 170°C (27).
Intensity of diffraction peaks in Fig. 4a becomes lower with CAB content, which is due to the partial restriction imposed by CAB on PVDF crystallization, as can be appreciated on the change of CI (Table 1 and Fig. 4b). This parameter was calculated as follows (28): $CI = (A_{crys.}/A_{tot.})x100$, where $A_{crys.}$ and $A_{tot.}$ are the area of peaks and the total area under the WAXS diffractogram, respectively. The change on CI (Table 1) for heated blends qualitatively agrees with the lowering of T_m and ΔH_f observed on DSC thermograms (Figs. 3a,b). Although PVDF crystallizes in higher extent in blends after heated than in those cast from DMF, the CI decreases drastically with CAB content in blends after heating and cooling to room temperature.
FTIR spectroscopy has proved to be extremely useful to follow the transformation from one crystalline phase into another in PVDF (6,7,9,10). Though the IR bands at 795 cm^{-1} (α-crystal form absorption) and at 840 cm^{-1} (β-crystal form absorption) have been used in the interpretation of IR studies on PVDF (29), the 550-450 cm^{-1} region seems to be the most suitable to identify α, β, γ forms, even when they are coexisting in the sample (9,10). Bands at 532 and 471 cm^{-1} are characteristic of the helical conformation TGTG (α-crystals) and of the planar zig-zag structure (β-crystals), respectively (9,10). Also, the lack of this bands and the absorption bands at 511 and 484 cm^{-1} indicate the presence of γ-crystals.
As observed in Fig. 5a, the bands at 511 and 484 cm^{-1} (γ-crystals) are predominant in the FTIR spectrum of pure PVDF, and those at 532 and 490 cm^{-1} (α-crystals) have a very low intensity. The lack of the band at 471 cm^{-1} in the as-cast PVDF spectrum indicates the absence of β-crystals. This observation concurs with that already reported for PVDF films cast from DMF yielding γ-crystals (22). For the as-cast blends, the band at 490 cm^{-1} appears higher in intensity and that at 484 cm^{-1} becomes a shoulder. As CAB content is increased, bands at 511 and 484 cm^{-1} (γ-crystals) decrease, whereas those at 532 and 490 cm^{-1}(α-crystals) remain almost constant in intensity. Thus, it is not clear what may be the origin of the peak at 206°C observed in the first DSC traces of PVDF/CAB blends. However, taking into account the results reported by Morra and Stein (22), one can speculate on the possibility for the formation of small amounts of γ′-crystals of PVDF due to the presence of CAB. These authors have found, from annealing experiments on PVDF/PMMA blends, that the melting point for different types of crystals follows the order: $\alpha < \gamma < \gamma'$, with the γ′ form being the highest one at 192°C, which is near to 206°C, observed here. Furthermore, Osaki and Ishida have observed that γ′ crystals, with a melting point as high as 199°C, result after annealing PVDF at 185.8°C (27). In light of these findings, it may be assumed that CAB induces the formation of γ′ crystals in cast blends, which would be a very uncommon effect, since this crystalline form has been stated to arise from solid-solid transformation of α phase. Thus, this peak needs to be more systematically studied.

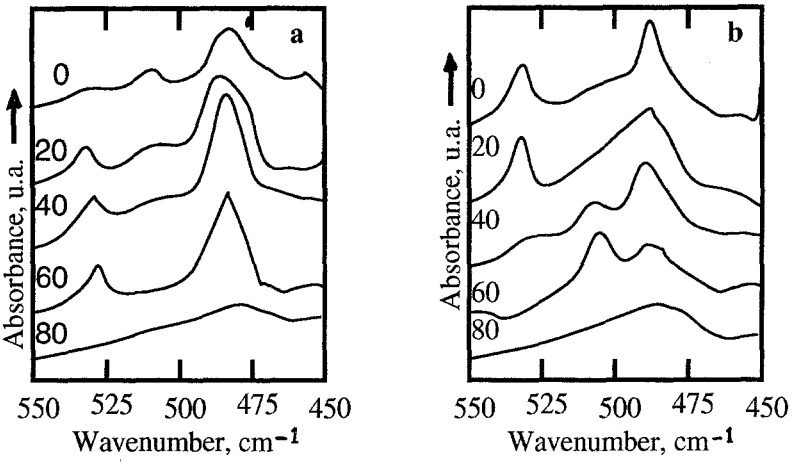

Fig. 5. FTIR spectra of the PVDF/CAB blends in the 450 - 550 cm^{-1} region: (a) before thermal treatment, and (b) after thermal treatment at 200°C for 30 min. Numerals indicate wt. % of CAB in blends.

Figure 5b reports IR spectra of PVDF/CAB blends after thermal treatment at 200°C for 30 min. The bands due to α-crystals at 532 and 490 cm^{-1} increased in intensity for PVDF and for the blend containing 20 wt. % of CAB. However, for higher contents of CAB (40 to 60 wt. %) the thermal treatment caused the band at 532 cm^{-1} (α-crystals) to vanish and that at 511 cm^{-1} (γ-crystals) to markedly increase in height. These results lead to the conclusion that the thermal treatment allows these blends to recover practically all the original amount of γ-crystals previously observed for the as-cast blends (Fig. 5a) of intermediate composition.This unexpected result indicates that CAB favors the transition of α to γ form during crystallization of PVDF from melt, and allows us to suspect that there is a significant polar interaction between CAB and PVDF, when both polymers are in the liquid state. This interaction may be similar to that taking place between PVDF and polar solvents as DMF or DMAc. A similar increase, but on β form, has been reported for PVDF/PVF blends containing about 10 wt. % of PVF (25).

Conclusions

According to DSC results, PVDF/CAB blends are partially miscible, exhibiting two composition-dependent T_g´s. Also, a decrease was observed on both the T_m and the ΔH_f of PVDF with the CAB content, which agrees with the partial miscibility assumed for this system. Similar behavior was observed for crystallinity index, as expected. WAXS and FTIR results indicated that PVDF, either pure or blended with CAB, crystallized predominantly in γ form, with a low amount of α form, when cast from DMF. Almost all the γ form was

transformed into the α form with the first DSC run, but it was recovered by thermal treatment at 200°C for blends of intermediate composition. Thus, CAB favors the formation of γ crystals in PVDF in the liquid state.

References

1 Lando JB, Olf HG, Peterlin A (1966) J. Polym. Sci. A-1, 4: 941
2 Takahashi Y, Kohyama M, Tadokoro H (1976) Macromolecules 9: 870
3 Lovinger AJ, Keith HD (1979) Macromolecules 12: 919
4 Lovinger AJ (1980) Polymer 21: 1317
5 Prest WM, Luca DJ (1975) J. Appl. Phys. 46: 4136
6 Lovinger AJ (1982) Macromolecules 15: 40
7 Takahashi Y, Matsubara Y, Tadokoro H (1982) Macromolecules 15: 334
8 Kobayashi M, Tashiro K, Tadokoro H (1975) Macromolecules 8: 158
9 Bachmann MA, Gordon WL, Koenig JL, Lando JB (1979) J Appl Phys 50:6106
10 Benedetti E, D´Alessio A, Bertolutti C, Vergamini P, Del Fanti N, Pianca M, Moggi G (1989) Polym Bull 22: 645
11 Cebe P, Grubb DT (1984) Macromolecules, 17: 1370
12 Nishi T, Wang TT (1976) Macromolecules 9: 603
13 Bernstein RE, Paul DR, Barlow JW (1978) Polym Eng Sci 18: 683
14 Wahrmund DC, Berstein RE, Barlow JW, Paul DR (1978) Polym Eng Sci 18: 677
15 Roerdink E, Challa G (1980) Polymer 21: 1161
16 Paul DR, Barlow JW, Berstein RE, Wahrmund DC (1978) Polym Eng Sci 18: 1225
17 Morra BS, Stein RS (1982) J Polym Sci; Polym Phys Ed 20: 2243
18 Brode GL, Koleske JV (1972) J Macromol Sci; Chem 6: 1109
19 Hubbell DS, Cooper SL (1977) J Appl Polym Sci 21: 3035
20 Olabisi O, Robeson LM, Shaw MT (1979) Polymer-Polymer Miscibility, Academic, New York (Chap. 5)
21 Bakhshandchfar R, Marand H (1991) Bull Am Phys Soc 36: 794
22 Morra BS, Stein RS (1982) J Polym Sci; Polym Phys Ed 20: 2261
23 Briber RM, Khoury F (1993) J Polym Sci; Polym Phys Ed 31: 2253
24 Plans J, MacKnight JW, Karasz FE, (1984) Macromolecules 17: 1100 (1984).
25 Lee H, Salomon RE, Labes MM (1978) Macromolecules 11: 171
26 Loufakis K, Wunderlich B (1987) Macromolecules 20: 2474
27 Osaki S, Ishida Y (1975) J Polym Sci; Polym Phys Ed 13: 1071
28 Alexander LE (1979) X-Ray Diffraction Methods in Polymer Science. Krieger Publ. Co., Huntington, New York (Chap. 3)
29 Naegele D, Yoon DY, Broadhurst MG (1978) Macromolecules 11: 1297

Received: 20 July 1994/Revised version: 6 September 1994/
Accepted: 9 September 1994